PAPER

Green synthesis of graphene oxide (GO)-anchored Pd/Cu bimetallic nanoparticles using *Ocimum sanctum* as bio-reductant: an efficient heterogeneous catalyst for the Sonogashira cross-coupling reaction†

Samim Sultana,[a] Swapna Devi Mech,[a] Farhaz Liaquat Hussain,[b] Pallab Pahari, [b] Geetika Borah [*a] and Pradip K. Gogoi[*a]

To explore the synergism between two metal centers we have synthesized graphene oxide (GO) supported Pd/Cu@GO, Pd@GO and Cu@GO nanoparticles through bio-reduction of Pd(NO$_3$)$_2$ and CuSO$_4$·5H$_2$O using Tulsi (*Ocimum sanctum*) leaf extract as the reducing and stabilizing agent. The graphene oxide (GO) was obtained by oxidation of graphite following a simplified Hummer's method. The as-prepared nanomaterials have been extensively characterized by FTIR, powder X-ray diffraction (PXRD), HRTEM, TEM-EDS, XPS, ICP-AES and BET surface area measurement techniques. The morphological study of Pd/Cu@GO revealed that crystalline bimetallic alloy type particles were dispersed on the GO layer. The activity of Pd@GO, Cu@GO and Pd/Cu@GO as catalysts for the Sonogashira cross-coupling reaction have been investigated and it was found that the Pd/Cu@GO nanostructure showed highly superior catalytic activity over its monometallic counterparts, substantiating the cooperative influence of the two metals. The inter-atom Pd/Cu transmetalation between surfaces was thought to be responsible for its synergistic activity. The catalyst showed higher selectivity towards coupling of aryl iodides with both aliphatic and aryl alkynes resulting in moderate to excellent isolated yield of the desired products (45–99%). The products have been characterized by GC-MS and ^{1}H-NMR spectroscopic techniques and compared with authentic samples. The Pd/Cu@GO catalyst could be easily isolated from the reaction products and reused for up to at least ten successive runs effectively.

1. Introduction

The palladium catalyzed Sonogashira cross-coupling reaction is one of the most powerful and reliable routes in modern synthetic organic chemistry for the formation of C sp^2–C sp bonds between aryl halides and terminal alkynes.[1] Aryl alkynes are versatile intermediates in the synthesis of natural products, pharmaceuticals, and agro-chemicals and in materials science. The traditional methods of Sonogashira cross-coupling reaction use an organic solvent such as an amine, benzene, acetonitrile, THF, DMSO or DMF with a palladium catalyst and a copper co-catalyst (enhancing the reaction efficiency) in the presence of

toxic phosphine or other ligands and a stoichiometric amount of base under inert conditions, which make it economically and environmentally malignant. Additionally, the use of copper as co-catalyst exhibits several drawbacks such as generation of Hay/Glaser type homo-coupling products of terminal alkynes along with the desired coupling product, thereby decreasing the efficiency of its formation.[2–6] On the other hand, a few successful examples of copper-free Sonogashira coupling require expensive aminophosphine ligands.[7] A large number of reports on the Sonogashira reaction used homogeneous palladium catalysts, while comparatively advantageous heterogeneous palladium catalysts have received less attention. The difficulties with the homogeneous catalysis are the isolation of the catalyst from the products and incapability of its application in the consecutive runs. Hence the necessity of heterogeneous approaches is highly preferred from the perspective of easy handling, easy catalyst separation and reusability.[4,5,8–11]

It is well-known that catalysis takes place on metal surface and nanoparticles (NPs) are much more reactive due to their small sizes and large surface areas than the particulate metal counterpart. As a result, heterogeneous catalysts in the form of

[a]*Department of Chemistry, Dibrugarh University, Dibrugarh-786004, Assam, India. E-mail: samimsultana786@gmail.com; swapnadevimech@gmail.com; flhussain786@gmail.com; ppahari@gmail.com; geetikachem@yahoo.co.in; pradip54@gmail.com*

[b]*Applied Organic Chemistry Group, Chemical Science and Technology Division, CSIR-North East Institute of Science and Technology, Jorhat-785006, Assam, India*

† Electronic supplementary information (ESI) available. See DOI: 10.1039/d0ra01189d

nanoparticles have gained tremendous importance in the fields like catalysis. In recent years, graphene and its derivatives have attracted the attention of researchers all over the world due to their unique two-dimensional structure, huge surface area, high dispersibility and other excellent properties.[12] Because of their inertness, large surface area, availability and stability, the chemically derived graphene such as graphene oxide (GO) and reduced graphene oxides (rGO) serve as ideal candidates as support in catalysis.[13] Several studies on catalysis using GO as support have been reported so far, *viz.* epoxidation of styrene,[14] aqueous phase Suzuki cross-coupling reaction,[12,15] Tsuji–Trost allylation,[16] hydrogenation of *p*-nitro phenol and hydrogen generation,[17] Sonogashira cross-coupling reaction[2] *etc.*

The bimetallic alloy nanoparticles comprising a noble metal with an additional cheaper (first-row transition) metal such as iron, cobalt, nickel and copper is an effective and low cost suitable alternative showing synergistic catalytic effects between the two distinct metals thereby decreasing the precious metal loading.[2,18] Despite a number of reports on bimetallic nanoparticles, palladium (with high surface-to-volume ratio, highly active surfaces, unique size, shape-dependent optoelectronic and anti-cancer properties)[19] and copper (super strong materials, with antibacterial, antifungal, sensing capacity, interaction with other nanoparticles due to the high surface area–volume ratio)[20,21] bimetallic nanoparticles have received significant attention in the field of catalysis. There are several methods for the synthesis of metal nanoparticles using toxic and expensive chemicals. In the recent past, Sonogashira cross-coupling reaction with various heterogeneous bimetallic nanoparticles have been reported, such

as Pd–Ni on ZIF-8,[22] Pd–Cu nanoparticles on magnesium oxide,[23] hollow Pd–Fe nanospheric catalyst,[24] Cu–Pd on poly-4-vinyl-pyridine,[25] gold–copper ferrite nanoparticles on silica microparticles,[26] Pd–Cu on graphene quantum dots modified Fe_3O_4 nanoparticles,[27] hollow Pd–Co nanospheres,[6] Pd–Co nanoparticles on graphene,[28,29] Pd–Cu nanoparticles on macroporous ion-exchange resin,[7] Pd–Cu nano alloys on montmorillonite,[30] Pd–Co nanoparticles on polypropylenimine grafted graphene,[31] Pd–Au on carbon,[32] CuPd nanoparticles on reduced graphene oxide,[2] *etc.* However, most of the above mentioned protocols suffered from serious disadvantages, *viz.* tedious experimental procedure, long reaction times, use of expensive, harsh and toxic chemicals (*e.g.* hydrazine hydrate, sodium borohydride, dimethylformamide, ethylene glycol, surfactants, organic ligands *etc.*) and so on. Thus, from the standpoint of the reduction of environmental burdens and cost effectiveness, environmentally benign methods of nanoparticles synthesis are highly appealing.[19,33–35] Biosynthesis of metal nanoparticles using plant materials can be used without maintaining cell culture and can suitably be scaled to large-scale nanoparticle synthesis, that's why receiving apex priority over other biological methods.[36,37] Various plant extracts, such as Tulsi (*Ocimum sanctum*),[33,38] tea,[37] coffee,[39] *C. Camphora*,[40] Magnolia,[36] soyabean[41] *etc.* have been used for biosynthesis of Pd and Cu nanoparticles. Tulsi (*Ocimum sanctum*) is a traditional medicinal plant, readily available in various parts of India. Tulsi leaves mainly contain phenolic acids, alkaloids, flavonoids, polyphenols, terpenoids *etc.* having excellent reducing and stabilizing properties are responsible for the formation and stabilization of metal nanoparticles,
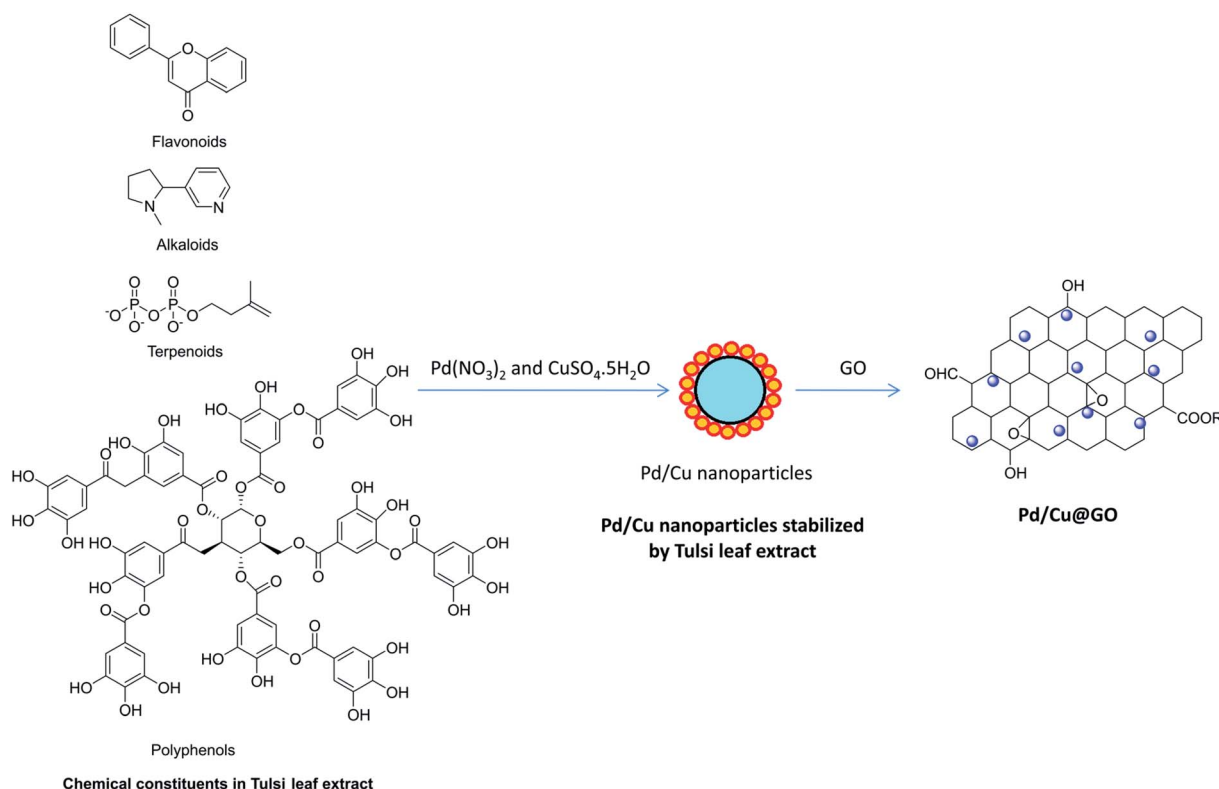
Scheme 1 Plausible reaction scheme for the components of plant extract for bio reduction of metal ions to nanoparticles.

respectively.[38,42] The tentative reaction scheme for the synthesis of Pd/Cu@GO nanocomposite through bio-reduction process by the components of Tulsi plant extract has been shown in Scheme 1.[43]

As per our knowledge, there is a single report of green synthesis of Pd@Fe$_3$O$_4$ nanoparticles and its application in Sonogashira cross-coupling reaction[44] however, it was associated with low fault, such as, long reaction time (24 h), use of high reaction temperature, toxic solvent, inert reaction medium *etc.* Contrastingly, there is no report available till date for the synthesis of bio-reduced graphene oxide supported bimetallic Pd/Cu nanocomposite and investigation of its heterogeneous catalytic potentiality in Sonogashira cross-coupling reaction in ethanol. From this point of view and in continuation of our previous works as well,[33,45–49] here we report the synthesis and characterization of ligand-free, Pd–Cu bimetallic nanoparticles supported on graphene oxide by bio reduction method and its application in Sonogashira cross-coupling reaction.

2. Experimental

2.1 General information

The chemicals used for the synthesis are of analytical reagent grade. All the chemicals were obtained commercially and were used as received without further drying or purification. Graphite was obtained from Otto, Biochemika; H$_2$SO$_4$, KMnO$_4$ were received from Fine Chemical Ltd. (Finer). Phenyl acetylene, 1-hexyne, 4-ethynyltoluene, 3-iodotoluene, 4-iodotoluene, bromobenzene, 4-bromotoluene, 4-bromoanisole, 4-bromoaniline and 1-iodo-3-nitrobenzene were purchased from Sigma-Aldrich. 4-ethynylanisole, 3-ethynylaniline, iodobenzene, CuSO$_4$, NaOH, K$_2$CO$_3$, NaNO$_3$, Pd(NO$_3$)$_2$, NaHCO$_3$, Et$_3$N and H$_2$O$_2$ were procured from different firms, such as TCI (Tokyo Chemical Industry), Merck Specialities, Lobachemic, Research-Lab Fine Chem. Industries, Spectrochem, Rankem *etc.*

FT-IR spectra were recorded in KBr pellets in a Shimadzu IR prestige-21 FT-IR spectrophotometer (400–4000 cm^{-1}). Powder X-
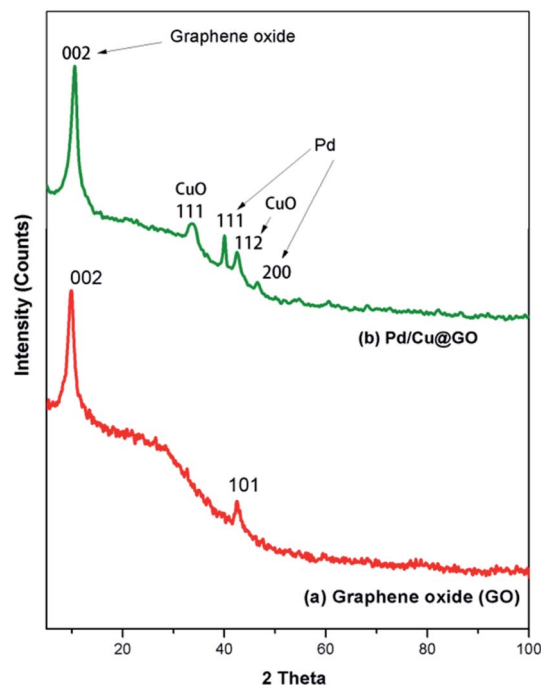
Fig. 2 XRD patterns of (a) GO and (b) Pd/Cu@GO.

ray diffraction (PXRD) patterns were recorded on a Rigaku Ultima IV diffractometer with Cu-K$_\alpha$ ($\lambda = 1.541$ Å radiation). TEM micrographs were obtained from SAIF, NEHU, Shillong using JEM-100 CX II and CSIR-NEIST, Jorhat using JEM-2100 Plus Electron Microscope. X-ray photoelectron spectrum (XPS) was performed at CSIR-NEIST, Jorhat using ESCALAB Xi+. Inductively Coupled Plasma Atomic Emission Spectrometric (ICP-AES) analyses were obtained from SAIF, IIT Bombay on ARCOS, Simultaneous ICP Spectrometer. The Brunauer–Emmett–Teller (BET) surface area measurements at liquid nitrogen temperature were recorded at BIT, Bangalore on Quantachrome Novae 2200. GC-MS of the products were performed on Agilent Technologies GC system 7820
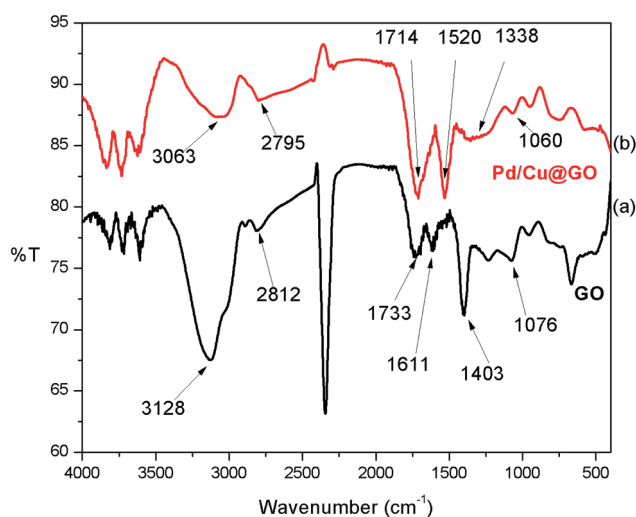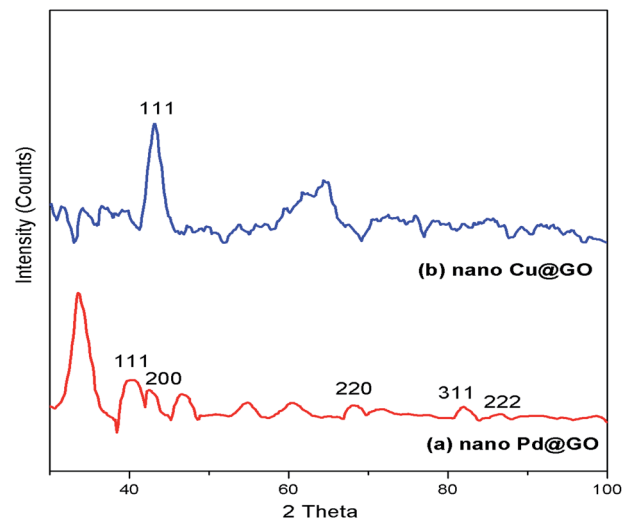
Fig. 1 FTIR spectra of (a) GO and (b) Pd/Cu@GO.

Fig. 3 XRD patterns of (a) Pd@GO and (b) Cu@GO.

coupled with a mass detector 5975 and SHRXI-5MS column. ^{1}H NMR spectra of the products were recorded in $CDCl_3$ using TMS as the internal standard using Bruker Ascend 500 MHz spectrometer.

2.2 Methods

2.2.1 Synthesis of graphene oxide (GO) from graphite (simplified Hummer's method). Graphene oxide (GO) was synthesized from oxidation of graphite.[50,51] In this method, graphite powder (5 g) and $NaNO_3$ (2.5 g) were mixed with H_2SO_4 (95%, 120 mL) in a 500 mL round bottom flask and stirred in an ice bath (0–5 °C) for 30 min. $KMnO_4$ (15 g) was added very slowly to the suspension in a manner that the reaction temperature was maintained below 20 °C. The ice bath was then removed and the mixture was stirred for overnight until its color turns to hasty brown. To the mixture, 150 mL of water was added slowly and the reaction temperature was maintained at 98 °C for one day. H_2O_2 (30%, 50 mL) was added slowly to the resulting mixture, whereupon color of the solution turns to bright yellow.
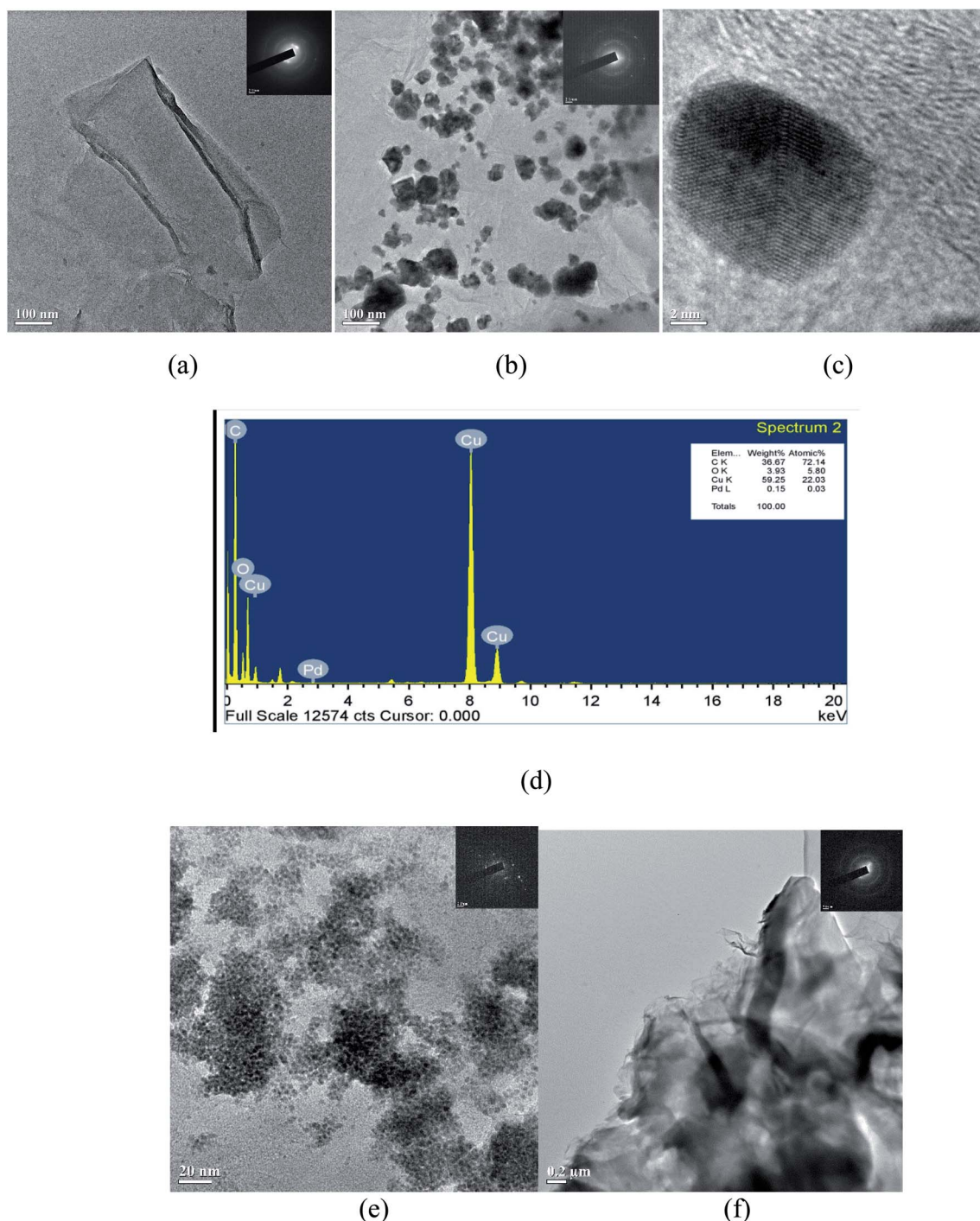

Fig. 4 TEM images of (a) GO and (b and c) Pd/Cu@GO with SAED patterns inset and (d) TEM-EDS (e) Pd@GO with SAED (f) Cu@GO with SAED.
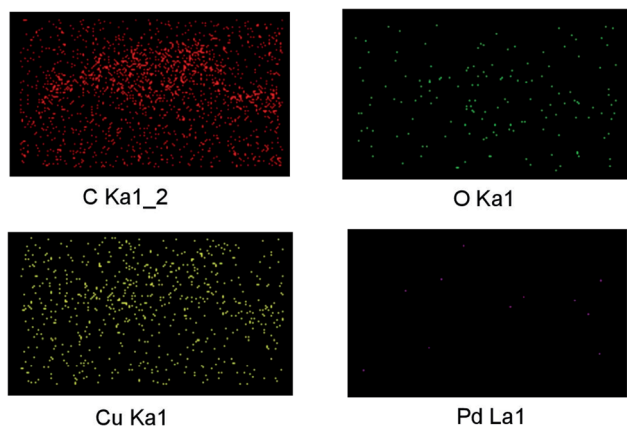
Fig. 5 Elemental dot mapping of Pd/Cu@GO nanocomposite.

It was purified by washing through centrifugation with 5% HCl followed by deionized water for several times. It was then dried in vacuum oven at room temperature and graphene oxide was obtained as powder.

2.2.2 Synthesis of Pd/Cu nanoparticles. A mixture of aqueous solution of 0.05 N $Pd(NO_3)_2$ (0.23 g $Pd(NO_3)_2$ in 40 mL water) and 0.05 N $CuSO_4 \cdot 5H_2O$ (0.249 g $CuSO_4 \cdot 5H_2O$ in 40 mL water) was taken in a round bottomed flask and stirred for 30 min. After that, 5 g of Tulsi (*Ocimum sanctum*) leaves were collected, washed thoroughly with distilled water, dried using blotting paper, crushed in a mortar, boiled in 50 mL water for 5 min, centrifuged and the filtrate was collected as the leaf extract. 6 mL of as-prepared leaf extract was added to the solution containing $Pd(NO_3)_2$ and $CuSO_4 \cdot 5H_2O$, allowed to stand for 5 min followed by stirring at room temperature for one day. The resulting mixture was centrifuged and the nanoparticles were collected.

2.2.3 Synthesis of graphene oxide anchored Pd/Cu nanocomposite (Pd/Cu@GO). To the suspension of Pd/Cu nanoparticles in water, 4 g of graphene oxide was added and the mixture was stirred for 6 days. After 6 days, the mixture was centrifuged, washed with water and acetone successively for several times and dried in air at room temperature. The product obtained was characterized and its application was studied.[33]
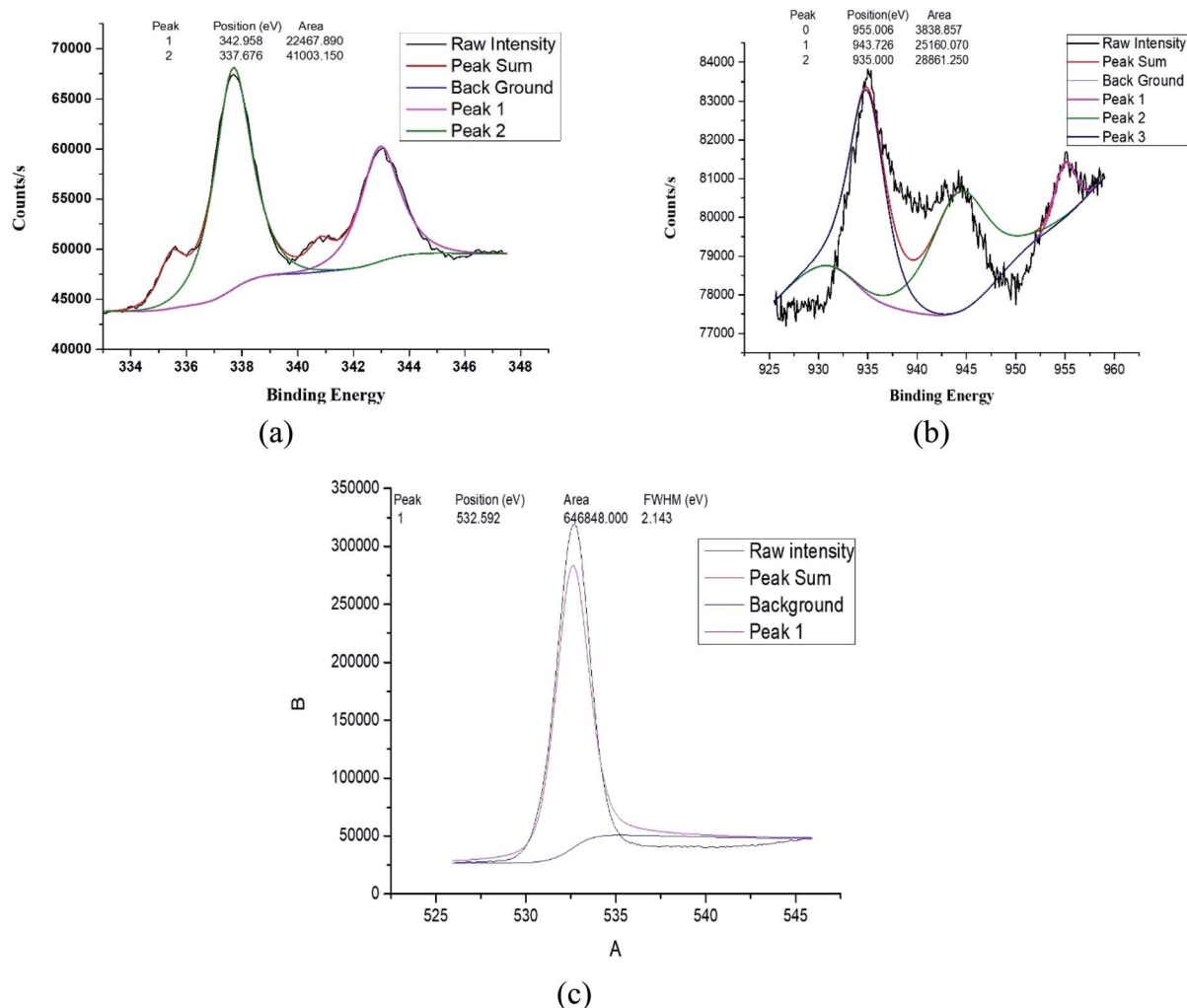

Fig. 6 (a) Deconvoluted high-resolution XPS spectrum of Pd 3d core level (b) deconvoluted high-resolution XPS spectrum of Cu 2p core level and (c) deconvoluted high-resolution XPS spectrum of O_{1s} core level for Pd/Cu@GO catalyst.
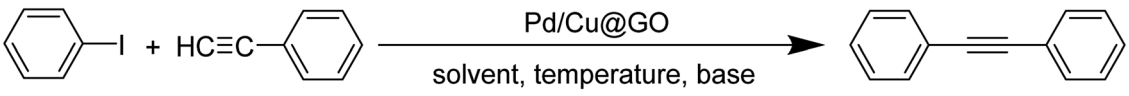
2.2.4 General procedure for Sonogashira cross-coupling reaction using Pd/Cu@GO catalyst. A mixture of aryl halide (1 mmol), alkyne (1 mmol), Et_3N (10 mL), ethanol (10 mL) and 5 mg of the catalyst (0.0001176 wt% Pd and 0.0002515 wt% Cu) was taken in a 25 mL round bottomed flask and was vigorously stirred at 75 °C for the required time. The progress of the reaction was monitored by TLC (Thin Layer Chromatography) using hexane as the eluent at different intervals of time. As the reaction completes (monitored by GC-MS), the catalyst was separated from the reaction mixture by simple filtration. The filtrate was treated with water–ethyl acetate mixture (water-: ethyl acetate = 1 : 1), followed by washing with brine and dehydrated with anhydrous Na_2SO_4. To get the desired product, the residue was purified by silica gel chromatography using hexane as the eluent. While recycling the catalyst, after each cycle it was isolated from the reaction mixture by simple centrifugation, washed with water and ethyl acetate for several times and dried in an oven at 110 °C for overnight. The recovered catalyst was then subjected for next runs under identical reaction conditions.

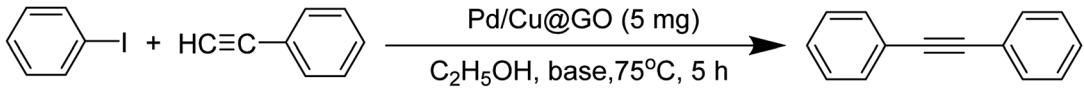**Table 1** BET surface area measurements of GO and Pd/Cu@GO nanocomposite

Serial no.	Materials	Surface area $(m^2\ g^{-1})$	Pore volume $(cc\ g^{-1})$	Pore diameter (nm)
1	GO	154	0.362	3.54
2	Pd/Cu@GO nanocomposite	374	0.507	1.49

Table 2 Optimization of reaction conditions for Sonogashira cross-coupling reaction of iodobenzene and phenyl acetylene[a]

Entry	Catalyst (amount in mg)	Base	Solvent	Time (h)	GC-MS (% conversion)	Isolated yield (%)
1	—	K_2CO_3	C_2H_5OH	24	—	—
2	5	K_2CO_3	C_2H_5OH	24	—	—
3	5	K_2CO_3	H_2O	24	—	—
4	10	K_2CO_3	C_2H_5OH	24	—	—
5	10	K_2CO_3	H_2O	24	—	—
6	10	K_2CO_3	C_2H_5OH	24	—	—[b]
7	10	K_2CO_3	H_2O	24	—	—[b]
8	10	K_2CO_3	C_2H_5OH	24	82	76[c]
9	10	K_2CO_3	H_2O	24	80	71[c]
10	5	Et_3N	H_2O	24	—	—[c]
11	3	Et_3N	C_2H_5OH	5	100	97[c]
12	**5**	**Et_3N**	**C_2H_5OH**	**5**	**100**	**99[c]**
13	10	Et_3N	C_2H_5OH	5	100	99[c]

[a] Reaction conditions: iodobenzene (1 mmol), phenyl acetylene (1 mmol), base (1 mmol/10 mL), solvent (10 mL), catalyst (Pd/Cu@GO, 0.0001176 wt% Pd and 0.0002515 wt% Cu), r.t. = 29 °C in air unless otherwise noted. [b] At 65 °C. [c] At 75 °C.

Table 3 Base optimization for Sonogashira cross-coupling reaction of iodobenzene and phenyl acetylene[a]

Entry	Base	GC-MS (% conversion)	Isolated yield (%)
1	**Et_3N**	**100**	**99**
2	NaOH	45	37
3	KOH	43	28
4	$NaHCO_3$	—	—
5	Na_2CO_3	—	—
6	K_2CO_3	71	63

[a] Reaction conditions: iodobenzene (1 mmol), phenyl acetylene (1 mmol), base (1 mmol/10 mL), solvent (ethanol, 10 mL), catalyst (Pd/Cu@GO, 0.0001176 wt% Pd and 0.0002515 wt% Cu), temperature = 75 °C.

3. Results and discussion

3.1 Characterization

3.1.1 FT-IR study. The FTIR spectrum of GO (Fig. 1a) shows significant peaks at 3128 and 2812 cm^{-1} corresponding to aromatic C–H and carboxylic acid O–H stretching vibrations, respectively. The peaks at 1733 and 1611 cm^{-1} could be attributed to anti-symmetric and symmetric stretching vibrations of carboxyl C=O respectively, while band at 1403 cm^{-1} could be assigned to C=C stretching vibration. The C–O–C stretching vibration appears at 1076 cm^{-1}.[52,53] The FTIR spectrum of Pd/Cu@GO (Fig. 1b) shows corresponding peaks with a clear downfield shift of $\Delta\nu = \sim16\text{–}91$ cm^{-1}, suggesting immobilization of Pd/Cu nanoparticles onto the GO sheet by some electrostatic interactions.[7]

3.1.2 XRD study. The crystalline nature of GO and Pd/Cu@GO can be confirmed from the powder X-ray diffraction patterns (Fig. 2). Fig. 2a shows the characteristic diffraction peaks of GO at $2\theta = 10.02°$ and $42.5°$ indicating insertion of oxygen rich functional groups within the graphite layers.[51,52,54] The broad peak between 20° and 30° could be assigned to disorderedly stacked graphene oxide.[55] The XRD pattern of Pd/Cu@GO exhibits characteristic diffractions of Pd (111) and (200) planes of face-centered cubic lattice at $2\theta = 40.07°$ and $46.7°$ (ref. 2 and 56) which were shifted from the reported 2θ values at 40.2° and 42.78° of Pd (111) and (200) planes, respectively.[2,57,58] Likewise, (111) and (112) planes of CuO have also been observed which shift to $2\theta = 33.62°$ and $42.72°$ from the reported value of 35.39° and 46.25°.[7] Moreover, on comparing the XRD pattern of Pd/Cu@GO (Fig. 2b) with that of Pd@GO [$2\theta = 40.2°$ (111), 42.78° (200), 67.9° (220), 82° (311) and 86.35° (222)][2,57,58] and Cu@GO [$2\theta = 42.89°$ (112)][20] (Fig. 3), it has been observed that in case of Pd/Cu@GO (Fig. 2b) the peaks undergoes some
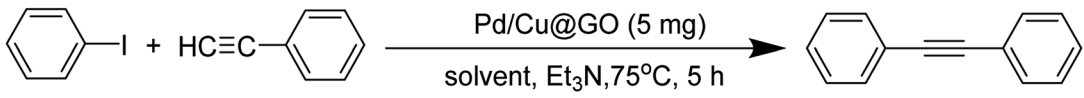
shifting. These observations are indicative of the presence of some type of interactions between Pd and Cu anchored on GO, rather than a physical mixture of Pd and Cu deposited on GO.

3.1.3 ICP-AES analysis. The ICP-AES analysis of the catalyst provided that our catalyst Pd/Cu@GO contains 0.0001176 wt% of Pd and 0.0002515 wt% of Cu.

3.1.4 HR-TEM analysis. The morphology and metal dispersion degree of GO and Pd/Cu@GO have been investigated with HR-TEM analysis (Fig. 4). The SAED patterns inset represent their crystallinity. The sheet like morphology of GO and the effective anchoring of Pd and Cu nanoparticles onto the surface of GO sheets are evident from their representative TEM micrographs (Fig. 4a and b). In the cross-sectional view of HRTEM image of Pd/Cu@GO (Fig. 4c), the crossing of interplanar fringes clearly indicates the presence of Pd and Cu as mixture rather than its monometallic counterparts. While comparing TEM images of Pd@GO and Cu@GO (Fig. 4e and f) with the catalyst (Fig. 4b) morphological changes were distinctly observed. Fig. 5 demonstrates the elemental dot mapping images indicating that Cu and Pd nanoparticles are homogeneously distributed throughout the surface of graphene oxide with Cu in higher weight% than that of Pd as observed from the TEM-EDS (Fig. 4d).

3.1.5 X-ray photoelectron spectroscopy (XPS) analysis. XPS measurements were done on Pd/Cu@GO nanocomposite to investigate the chemical state of Pd and Cu on the surface of the catalyst (Fig. 6). The core level spectrum for Pd 3d was characterized by a pair of relatively narrow peaks corresponding to the 5/2 and 3/2 spin–orbit components located at 337.68 and 342.96 eV, respectively could be assigned to Pd^0.[30,59,60] The Cu $2p_{3/2}$ and Cu $2p_{1/2}$ peaks at 935 eV and 955 eV, respectively were characteristic of Cu(II).[61] Additionally, the presence of Cu(II) could also be ascertained by the strong shake up peak observed

Table 4 Solvent screening for Sonogashira cross-coupling reaction of iodobenzene and phenyl acetylene[a]

Entry	Solvent	GC-MS (% conversion)	Isolated yield (%)
1	**C$_2$H$_5$OH**	**100**	**99**
2	H$_2$O	—	—
3	i-PrOH	89	81
4	CH$_3$OH	57	32
5	DCM	—	—
6	DMF	—	—
7	DMSO	—	—
8	CH$_3$CN	50	32
9	CHCl$_3$	—	—
10	CCl$_4$	—	—
11	C$_2$H$_5$OH	—	—[b]
12	C$_2$H$_5$OH	10	7[c]
13	C$_2$H$_5$OH	—	—[d]

[a] Reaction conditions: iodobenzene (1 mmol), phenyl acetylene (1 mmol), base (Et$_3$N, 10 mL), solvent (10 mL), catalyst (Pd/Cu@GO, 0.0001176 wt% Pd and 0.0002515 wt% Cu), otherwise noted. [b] GO. [c] Nano Pd@GO. [d] Nano Cu@GO, temperature = 75 °C.
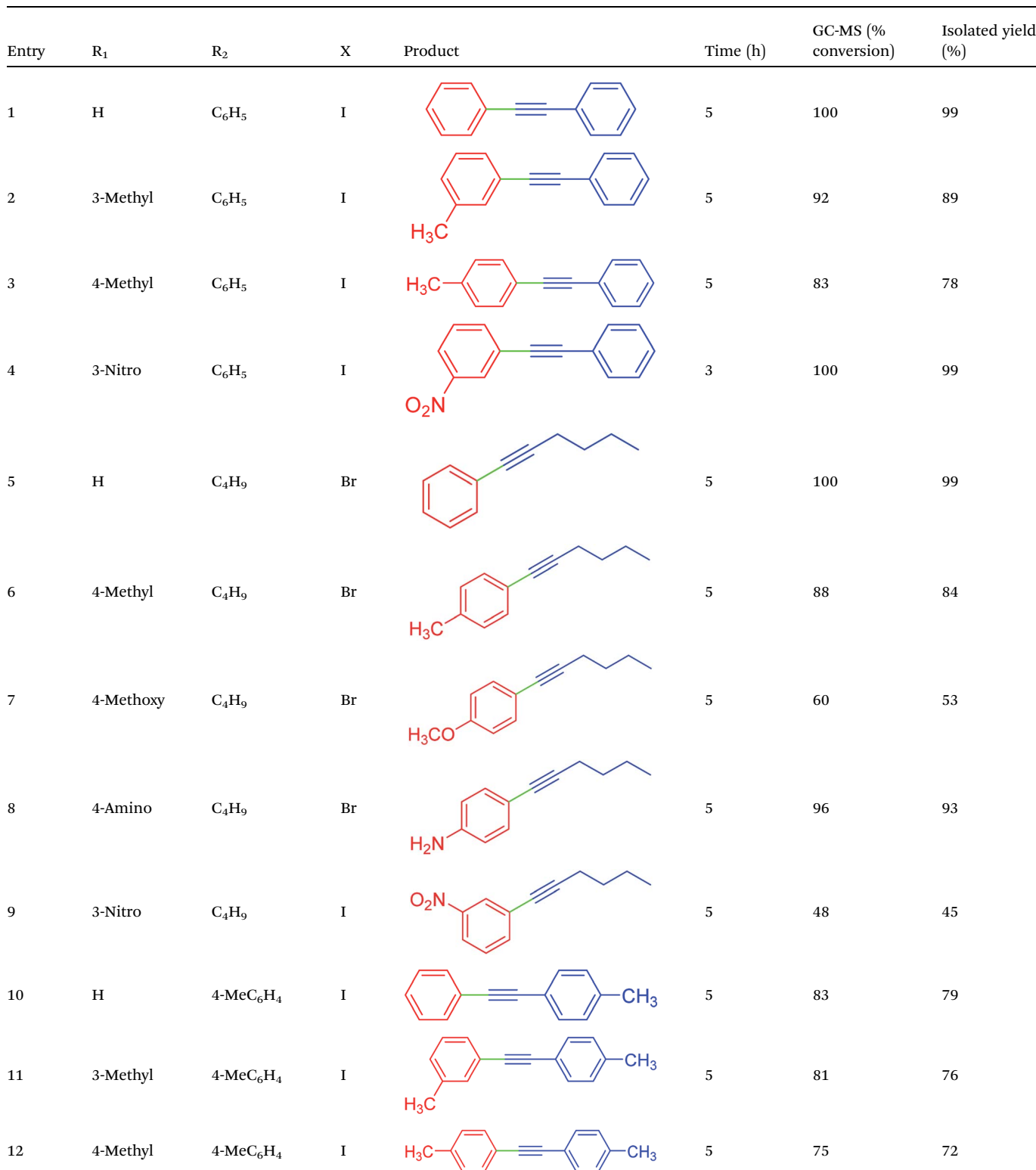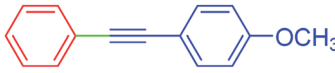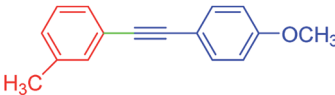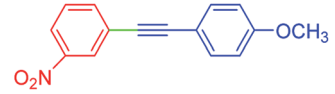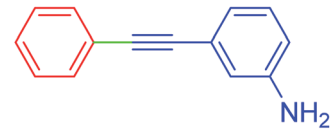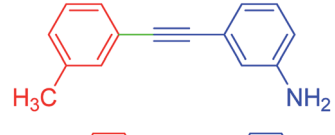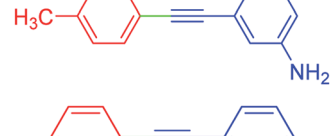
Table 5 Sonogashira cross-coupling reaction of various aryl halides and alkynes catalyzed by Pd/Cu@GO[a]

Entry	R_1	R_2	X	Product	Time (h)	GC-MS (% conversion)	Isolated yield (%)
1	H	C_6H_5	I		5	100	99
2	3-Methyl	C_6H_5	I		5	92	89
3	4-Methyl	C_6H_5	I		5	83	78
4	3-Nitro	C_6H_5	I		3	100	99
5	H	C_4H_9	Br		5	100	99
6	4-Methyl	C_4H_9	Br		5	88	84
7	4-Methoxy	C_4H_9	Br		5	60	53
8	4-Amino	C_4H_9	Br		5	96	93
9	3-Nitro	C_4H_9	I		5	48	45
10	H	4-MeC_6H_4	I		5	83	79
11	3-Methyl	4-MeC_6H_4	I		5	81	76
12	4-Methyl	4-MeC_6H_4	I		5	75	72

Table 5   (Contd.)

Entry	R$_1$	R$_2$	X	Product	Time (h)	GC-MS (% conversion)	Isolated yield (%)
13	H	4-MeOC$_6$H$_4$	I		5	76	71
14	3-Methyl	4-MeOC$_6$H$_4$	I		5	63	57
15	4-Methyl	4-MeOC$_6$H$_4$	I		5	72	68
16	3-Nitro	4-MeOC$_6$H$_4$	I		5	97	91
17	H	3-NH$_2$C$_6$H$_4$	I		5	63	57
18	3-Methyl	3-NH$_2$C$_6$H$_4$	I		5	61	54
19	4-Methyl	3-NH$_2$C$_6$H$_4$	I		5	60	53
20	3-Nitro	3-NH$_2$C$_6$H$_4$	I		5	73	65

[a] Reaction conditions: aryl halide (1 mmol), alkyne (1 mmol), base (Et$_3$N, 10 mL), solvent (ethanol, 10 mL), catalyst (Pd/Cu@GO, 0.0001176 wt% Pd and 0.0002515 wt% Cu), temperature = 75 °C.

at 943.7 eV.[61,62] A clear shifting of Cu 2p$_{3/2}$ peak to higher binding energy (935 eV) in the as-synthesized catalyst might be due to the formation of Cu–O–C type surface structure.[62] The O$_{1s}$ spectrum showed a peak at 532.6 eV with a shift of ∼2 eV towards higher binding energy. This component might be due to the presence of metal–oxygen bond and may be attributed to small particle with a higher number of defect sites and low oxygen coordination.

3.1.6   Surface area measurement. The BET surface area, pore volume and pore diameter of GO and Pd/Cu@GO nanocomposite are shown in Table 1. It has been observed that upon immobilization of Pd and Cu nanoparticles onto the surface of GO its surface area and pore volume increased, making it a good

candidate for adsorption of the reactant molecules over its surface indicating enhanced catalytic activity.[63]

4.   Sonogashira cross-coupling reaction catalyzed by Pd/Cu@GO nanocomposite

In order to obtain the best reaction condition, we have chosen iodobenzene and phenyl acetylene as the model substrates and have conducted a series of reactions under different conditions as presented in Table 2. First of all, in absence of any catalyst, iodobenzene (1 mmol), phenyl acetylene (1 mmol), K$_2$CO$_3$ (base,

L = Ligand from GO
R₁ = substituted/ unsubstituted aryl group
R₂ = aryl/alkyl group
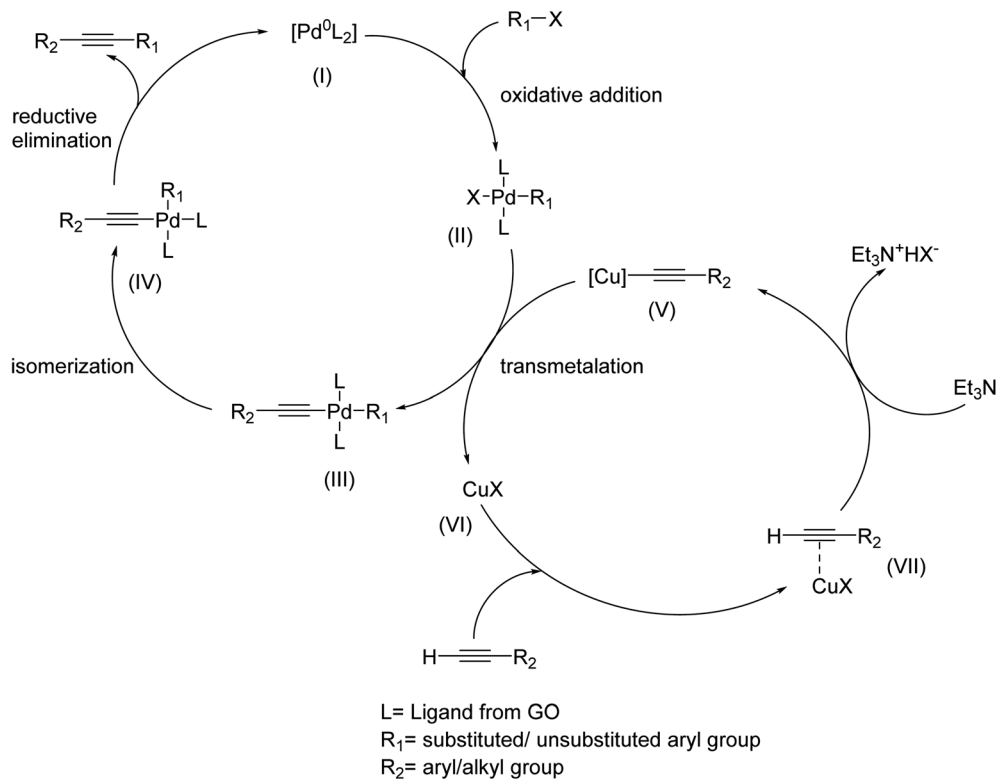
Scheme 2 Plausible mechanism for Sonogashira cross coupling reaction.

Table 6 Comparison of catalytic activity of our catalyst (Pd/Cu@GO) with previously reported Pd–Cu based catalysts for Sonogashira cross-coupling reaction

Entry	Catalyst	Substrates	Temperature reaction condition	Reaction time (h) (reusability)	Solvent	Isolated yield (%)	Reference
1	Pd/Cu@GO	Aryl iodides and bromides with aliphatic and aromatic terminal alkynes	75 °C magnetic stirring	3–5 (10 cycles)	Ethanol	45–99	Author's present work
2	rGO–CuPd	Aryl iodides and bromides with phenyl acetylene	120 °C magnetic stirring	1–5 (5 cycles)	DMF	70–96	2
3	Pd/Cu–ARF(II)	Aryl iodides and bromides with aliphatic and aromatic terminal alkynes	80 °C magnetic stirring N₂ atmosphere	3–16 (5 cycles)	CH₃CN	77–95	7
4	MgO@PdCu	Aryl iodides, bromides and chloride with aliphatic and aromatic terminal alkynes	60–120 °C magnetic stirring	6–24 (11 cycles)	DABCO and DMF	10–99	23
5	MMT@Pd/Cu	Aryl iodides with aliphatic and aromatic terminal alkynes	65 °C magnetic stirring N₂ atmosphere	16	Ethanol	57–97	30
6	PdCu@GQD@Fe₃O₄	Aryl iodides, bromides and chloride with aromatic terminal alkynes	50–110 °C	8–48 (10 cycles)	DABCO, toluene or DMA	76–99	37
7	Pd–CuFe₂O₄@SiO₂	Aryl iodides and bromides with aromatic terminal alkynes	50 °C	24 (5 cycles)	DABCO, DMA	68–98	67

1 mmol) and ethanol (solvent, 10 mL) were taken and carried out the reaction for 24 h which did not lead to any product formation (Table 2, entry 1). Introduction of the catalyst at room temperature also showed no product formation (Table 2, entries 2–5). Even increase in temperature to 65 °C did not afford any positive results (Table 2, entries 6 & 7). But it delighted us when increasing the temperature to 75 °C gave 76 and 71% isolated yield of products (Table 2, entries 8 & 9). This showed that both
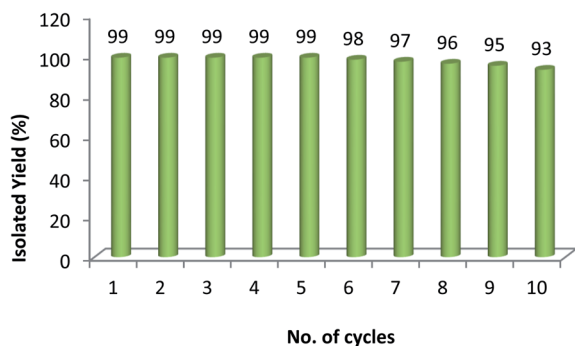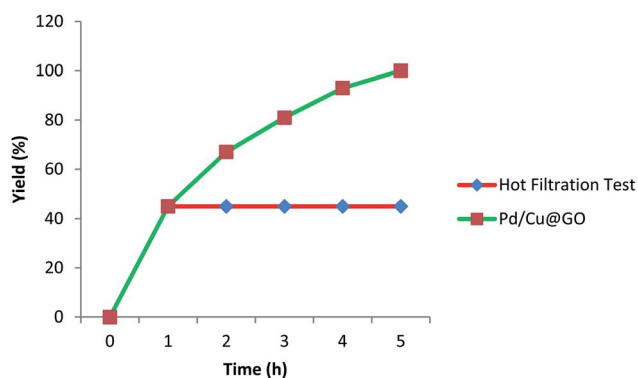
Fig. 7 Recycling of the catalyst.

Fig. 8 Hot Filtration Test.

temperature and amount of catalyst played an important role in this reaction (Table 2, entries 11–13). Hence, 5 mg of the catalyst at 75 °C was found to be the suitable amount to carry out the reaction effectively.

As base is an inevitable part for Sonogashira cross-coupling reaction, we have performed the reaction in presence of a number of bases as shown in Table 3. Our investigations showed that Et$_3$N acts as the most suitable base for this reaction (Table 3, entry 1).

Solvent screening with a number of solvents showed ethanol is the best solvent in this case. The DMF, DMSO and CH$_3$CN are capable of coordinating as a ligand with the metals and thereby, the stability of the catalyst might be affected by competing with the ligands. Moreover, since our catalytic system contains Cu as Cu^{2+}, therefore, during catalytic reactions Cu^{2+} must be reduced to Cu$^+$ by some means (Cu$^+$ is the active species to carry out Sonogashira reaction). Therefore, ethanol featuring a reducing property is most effective in our case (Table 4, entry 1). Our investigations showed that 5 mg of the catalyst (Pd/Cu@GO, 0.0001176 wt% Pd and 0.0002515 wt% Cu) at 75 °C in Et$_3$N (10 mL) and ethanol (10 mL) is the best reaction condition for this reaction. It is noteworthy to mention that we have synthesized Pd@GO and Cu@GO following the same synthetic procedure as described for Pd/Cu@GO nanocomposite and examined their catalytic efficiency too for the said reaction under the identical optimized condition (Table 4, entries 12 and 13). These results clearly demonstrated that Pd/Cu@GO

nanostructure showed highly superior catalytic activity over its monometallic counterparts, substantiating the presence of some type of cooperative influence between Pd and Cu.

The scope and limitations of Pd/Cu@GO were studied with various aryl halides and alkynes under the optimized reaction condition (Table 5). Our results showed that coupling of phenyl acetylene with aryl iodides bearing electron donating group (–CH$_3$) afforded lower yields (Table 5, entries 2 and 3) compared to that bearing electron withdrawing group (–NO$_2$) (Table 5, entry 4). This might be due to the increase of electron density around the aromatic ring making it difficult to remove the iodo-group from the substrate.[2] It is remarkable to note that coupling of phenyl acetylene with aryl bromides for 8 h duration resulted no product formation, while coupling of 1-hexyne with aryl bromides gave noticeable isolated yields (Table 5, entries 5–8).We have examined a series of coupling reactions between 1-hexyne with aryl iodides, and interestingly only nitro derivative can afford product formation with moderate isolated yield (Table 5, entry 9). In contrast to that, 4-ethynyltoluene, 4-ethynylanisole and 3-ethynylaniline gave good isolated yields when coupled with aryl iodides (Table 5, entries 10–20), while with aryl bromides did not lead to product formation.

4.1 Probable mechanism

The plausible mechanism for Sonogashira cross-coupling reaction follows the pathway[64,65] as shown in Scheme 2. In the first step, oxidative addition of aryl halide with the active Pd species (I) takes place to generate the species (II). Cu(II) is *in situ* reduced to Cu(I) in the presence of reducing solvent (ethanol) and reducing components of plant extract. Cu(I) activates the terminal alkyne by generating transient alkynyl copper intermediate which facilitates the transmetalation with the previously formed species (II) to give (III). The desired coupled product is obtained by isomerization of (III) followed by reductive elimination of (IV).

The present catalytic system appears to be more efficient in the Sonogashira reaction for several reasons: (i) use plant extract instead of toxic chemicals as the reducing agents, (ii) does not release any toxic bi-products into the environment, (iii) cost effective, (iv) use of mild reactions conditions, completely ligand free, no additional co-catalyst is required, and (v) the catalyst is recyclable without any apparent leaching.[19,66] Table 6 highlighting the improved catalytic performance and reaction conditions as well, of the present catalytic protocol compared to that of similar Pd and Cu-based heterogeneously catalytic systems reported so far. To the best of our knowledge, our Pd/Cu@GO nanocomposite could provide highly attractive and environment friendly option for the synthesis of aryl alkynes.

4.2 Recycling of the catalyst

The reusability is the key parameter to evaluate the sustainability and efficiency of a heterogeneous catalyst. That is why we have carried out the recyclability of Pd/Cu@GO for Sonogashira cross-coupling reaction between iodobenzene and phenyl acetylene under the optimized reaction condition. After completion of the reaction, it was easily separated from the reaction mixture

by centrifugal precipitation, washed thoroughly with water and ethyl acetate and then dried. It was applied for subsequent runs and continued up to tenth cycle. The slight decrease in product yield after the fifth cycle might be indicative of very gradual catalyst deterioration. After all, the catalyst was found to be quite active even up to tenth cycle giving 93% isolated yield (Fig. 7).

In order to establish the heterogeneous nature of the catalyst, we have performed a hot filtration test (Fig. 8) using iodobenzene and phenyl acetylene as the model substrates under the optimized reaction condition. After 1 h, the reaction was stopped and the catalyst was filtered off from the reaction mixture. The percentage of product formation was analyzed with GCMS (45% conversion). The reaction was continued with the filtrate obtained (without any solid catalyst) for another 4 h and found no product formation (studied with GCMS), indicating non-leaching of metals during the catalytic cycle. Moreover, the ICP-AES analysis of the filtrate showed Pd or Cu content below detection level (*i.e.* <0.01 ppm) which further enumerates non-leaching of either Cu or Pd metal during the reactions, thereby affirming its heterogeneous nature and stability.

5. Conclusion

The present study reports a sustainable, green approach to integrate Pd with Cu on graphene oxide and exploiting its catalytic potency for Sonogashira cross-coupling reaction. The benign reaction conditions, use of bio-reducing agents and its easy availability, easy separability, excellent retrievability (at least for ten consecutive runs) attesting its superiority. Only 0.0001176 wt% Pd and 0.0002515 wt% Cu is sufficient to produce excellent isolated yields is the added advantage of Pd/Cu@GO catalyst. This bio-reduced, GO anchored Pd/Cu bimetallic nanocomposite catalytic protocol has been applied for the 1st time in Sonogashira cross-coupling reactions under ligand free, eco-friendly conditions. The remarkably high catalytic activity of Pd/Cu@GO over its monometallic counterparts (Pd@GO and Cu@GO) clearly demonstrating to the cooperative influence between Pd and Cu in the nanostructure.

Conflicts of interest

The authors declare that there is no conflict of interest regarding the publication of this article.

Acknowledgements

References

1 K. Ramesh and G. Satyanarayana, *J. Organomet. Chem.*, 2019, **890**, 58.

2 S. Diyarbakir, H. Can and O. Metin, *ACS Appl. Mater. Interfaces*, 2015, **7**, 3199.

3 S. K. Das, M. Sarmah and U. Bora, *Tetrahedron Lett.*, 2017, **58**, 2094.

4 Z. I. Dehimat, S. Yasar, D. Tebbani and I. Özdemir, *Inorg. Chim. Acta*, 2018, **469**, 325.

5 Y. B. Platonova, A. N. Volov and L. G. Tomilova, *J. Catal.*, 2019, **373**, 222.

6 H. Zhong, J. Wang, L. Li and R. Wang, *Dalton Trans.*, 2014, **43**, 2098.

7 D. Sengupta, J. Saha, G. De and B. Basu, *J. Mater. Chem. A*, 2014, **2**, 3986.

8 H. Li, Z. Zhu, J. Liu, S. Xie and H. Li, *J. Mater. Chem.*, 2010, **20**, 4366.

9 A. Komáromi, G. L. Tolnai and Z. Novák, *Tetrahedron Lett.*, 2008, **49**, 7294.

10 J. T. Guan, T. Q. Weng, G. A. Yu and S. H. Liu, *Tetrahedron Lett.*, 2007, **48**, 7129.

11 M. J. Mio, L. C. Kopel, J. B. Braun, T. L. Gadzikwa, K. L. Hull, R. J. Brisbois, C. J. Markworth and P. A. Grieco, *Org. Lett.*, 2002, **4**, 3199.

12 C. Bai, Q. Zhao, Y. Li, G. Zhang, F. Zhang and X. Fan, *Catal. Lett.*, 2014, **144**, 1617.

13 S. Sabater, J. A. Mata and E. Peris, *ACS Catal.*, 2014, **4**, 2038.

14 H. Su, Z. Li, Q. Huo, J. Guan and Q. Kan, *RSC Adv.*, 2014, **4**, 9990.

15 J. H. Park, F. Raza, S. J. Jeon, H. I. Kim, T. W. Kang, D. B. Yim and J. H. Kim, *Tetrahedron Lett.*, 2014, **55**, 3426.

16 Q. Zhao, Y. Zhu, Z. Sun, Y. Li, G. Zhang, F. Zhang and X. Fan, *J. Mater. Chem. A*, 2015, **3**, 2609.

17 W. Sun, X. Lu, Y. Tong, Z. Zhang, J. Lei, G. Nie and C. Wang, *Int. J. Hydrogen Energy*, 2014, **39**, 9080.

18 K. W. Cheah, M. J. Taylor, A. Osatiashtiani, S. K. Beaumont, D. J. Nowakowski, S. Yusup, A. V. Bridgwater and G. Kyriakou, *Catal. Today*, 2019, DOI: 10.1016/j.cattod.2019.03.017.

19 H. Veisi, A. Rashtiani and V. Barjasteh, *Appl. Organomet. Chem.*, 2016, **30**, 231.

20 J. Ramyadevi, K. Jeyasubramanian, A. Marikani, G. Rajakumar and A. A. Rahuman, *Mater. Lett.*, 2012, **71**, 114.

21 J. S. Cerda, H. E. Gómez, G. A. Núñez, I. A. Rivero, Y. G. Ponce and L. Z. F. López, *J. Saudi Chem. Soc.*, 2016, **21**, 341.

22 Y. Wang, Y. Zeng, X. Wu, M. Mu and L. Chen, *Mater. Lett.*, 2018, **220**, 321.

23 M. Gholinejad, M. Bahrami, C. Nájera and B. Pullithadathil, *J. Catal.*, 2018, **363**, 81.

24 H. Li, Z. Zhu, H. Li, P. Li and X. Zhou, *J. Colloid Interface Sci.*, 2010, **349**, 613.

25 C. Evangelisti, A. Balerna, R. Psaro, G. Fusini, A. Carpita and M. Benfatto, *ChemPhysChem*, 2017, **18**, 1921.

26 M. Gholinejad, J. Ahmadi and C. Nájera, *ChemistrySelect*, 2016, **3**, 384.

27 M. Gholinejad, J. Ahmadi, C. Najera, M. Seyedhamzeh, F. Zareh and M. K. Zareh, *ChemCatChem*, 2017, **9**, 1442.

28 Y. S. Feng, X. Y. Lin, J. Hao and H. J. Xu, *Tetrahedron*, 2014, **70**, 5249.

29 M. Dabiri and M. P. Vajargahy, *Appl. Organomet. Chem.*, 2017, **31**, e3594.

30 W. Xu, H. Sun, B. Yu, G. Zhang, W. Zhang and Z. Gao, *ACS Appl. Mater. Interfaces*, 2014, **6**, 20261.

31 A. Shaabani and M. Mahyari, *J. Mater. Chem. A*, 2013, **1**, 9303.

32 C. Rossy, J. Majimel, E. Fouquet, C. Delacote, M. Boujtita, C. Labrugere, M. T. Delapierre and F. X. Felpin, *Chem.–Eur. J.*, 2013, **19**, 14024.

33 N. Gogoi, P. Bordoloi, G. Borah and P. K. Gogoi, *Catal. Lett.*, 2017, **147**, 539.

34 S. Momeni and I. Nabipour, *Appl. Biochem. Biotechnol.*, 2015, **176**, 1937.

35 A. Kalaiselvi, S. M. Roopan, G. Madhumitha, C. Ramalingam and G. Elango, *Spectrochim. Acta, Part A*, 2015, **135**, 116.

36 H. J. Lee, G. Lee, N. R. Jang, J. H. Yun, J. Y. Song and B. S. Kim, *NSTI Nanotech*, 2011, **1**, 371.

37 S. Lebaschi, M. Hekmati and H. Veisi, *J. Colloid Interface Sci.*, 2017, **485**, 223.

38 V. D. Kulkarni and P. S. Kulkarni, *Int. J. Chem. Stud.*, 2013, **1**, 2321.

39 M. N. Nadagouda and R. S. Varma, *Green Chem.*, 2008, **10**, 859.

40 J. Huang, Q. Li, D. Sun, Y. Lu, Y. Su, X. Yang, H. Wang, Y. Wang, W. Shao, N. He, J. Hong and C. Chen, *Nanotechnology*, 2007, **18**, 105104.

41 J. I. Abd-Elkareem, H. M. Bassuony, S. M. Mohammed, H. M. Fahmy and N. R. Abd-Elkader, *J. Bionanosci.*, 2016, **10**, 15.

42 P. K. Saikia, R. P. Bhattacharjee, P. P. Sarmah, L. Saikia and D. K. Dutta, *RSC Adv.*, 2016, **6**, 110011.

43 M. Nasrollahzadeh, M. Sajjadi, J. Dadashi and H. Ghafuri, *Adv. Colloid Interface Sci.*, 2020, **276**, 102103.

44 M. Nasrollahzadeh, S. M. Sajadi, A. Rostami-Vartooni and M. Khalaj, *J. Mol. Catal. A: Chem.*, 2015, **396**, 31.

45 S. Sultana, G. Borah and P. K. Gogoi, *Appl. Organomet. Chem.*, 2019, **33**, e4595.

46 S. Sultana, G. Borah and P. K. Gogoi, *Catal. Lett.*, 2019, **149**, 2142.

47 S. Sultana, S. Bordoloi, S. Konwer, G. Borah and P. K. Gogoi, *Appl. Organomet. Chem.*, 2020, e5582.

48 R. Gogoi, R. Saikia and G. Borah, *J. Organomet. Chem.*, 2019, **897**, 80.

49 C. Pathak and G. Borah, *Mater. Res. Express*, 2019, **6**, 1250i1.

50 F. T. Thema, M. J. Moloto, E. D. Dikio, N. N. Nyangiwe, L. Kotsedi, M. Maaza and M. Khenfouch, *J. Chem.*, 2013, 150536.

51 N. Xiang, J. Huang, H. Zhao, C. Liu and X. Liu, *Z. Phys. Chem.*, 2016, **230**, 1711.

52 C. Ma, K. Yang, L. Wang and X. Wang, *J. Appl. Biomater. Funct. Mater.*, 2017, **15**, 1.

53 N. Hussain, P. Gogoi, P. Khare and M. R. Das, *RSC Adv.*, 2015, **5**, 103105.

54 H. Yang, J. Jiang, W. Zhou, L. Lai, L. Xi, Y. M. Lam, Z. Shen, B. Khezri and T. Yu, *Nanoscale Res. Lett.*, 2011, **6**, 531.

55 N. Shang, C. Feng, H. Zhang, S. Gao, R. Tang, C. Wang and Z. Wang, *Catal. Commun.*, 2013, **40**, 111.

56 G. Wu, X. Wang, N. Guan and L. Li, *Appl. Catal., B*, 2013, **136–137**, 177.

57 A. H. Al-Marri, M. Khan, M. R. Shaik, N. Mohri, S. F. Adil, M. Kuniyil, H. Z. Alkhathlan, A. Al-Warthan, W. Tremel, M. N. Tahir, M. Khan and M. R. H. Siddiqui, *Arabian J. Chem.*, 2016, **9**, 835.

58 W. Sun, X. Lu, Y. Tong, Z. Zhang, J. Lei, G. Nie and C. Wang, *Int. J. Hydrogen Energy*, 2014, **39**, 9080.

59 X. Zhang, D. Wu and D. Cheng, *Electrochim. Acta*, 2017, **246**, 572.

60 M. K. Mohan, K. R. Sunajadevi, N. K. Daniel, S. Gopi, S. Sugunan and N. C. Perumparakunnel, *Bull. Chem. React. Eng. Catal.*, 2018, **13**, 286.

61 S. M. Lomnicki, H. Wu, S. N. Osborne, J. M. Pruett, R. L. McCarley, E. Poliakoff and B. Dellinger, *Mater. Sci. Eng., B*, 2010, **175**, 136.

62 T. Tsoncheva, G. Issa, T. Blasco, M. Dimitrov, M. Popova, S. Hernandez, D. Kovacheva, G. Atanasova and J. M. L. Nieto, *Appl. Catal., A*, 2013, **453**, 1.

63 S. Verma, R. B. N. Baig, M. N. Nadagouda and R. S. Varma, *Green Chem.*, 2016, **18**, 1327.

64 M. H. P. Temprano, J. A. Casares and P. Espinet, *Chem.–Eur. J.*, 2012, **18**, 1864.

65 R. Chinchilla and C. Nájera, *Chem. Rev.*, 2007, **107**, 874.

66 C. Ha, N. Zhu, R. Shang, C. Shi, J. Cui, I. Sohoo, P. Wu and Y. Cao, *Chem. Eng. J.*, 2016, **288**, 246.

67 M. Gholinejad and J. Ahmadi, *ChemPlusChem*, 2015, **80**, 973.